

PruneNet: Channel Pruning via Global Importance

Ashish Khetan
Amazon AWS
khetan@amazon.com

Zohar Karnin
Amazon AWS
zkarnin@amazon.com

Abstract

Channel pruning is one of the predominant approaches for accelerating deep neural networks. Most existing pruning methods either train from scratch with a sparsity inducing term such as group lasso, or prune redundant channels in a pretrained network and then fine tune the network. Both strategies suffer from some limitations: the use of group lasso is computationally expensive, difficult to converge and often suffers from worse behavior due to the regularization bias. The methods that start with a pretrained network either prune channels uniformly across the layers or prune channels based on the basic statistics of the network parameters. These approaches either ignore the fact that some CNN layers are more redundant than others or fail to adequately identify the level of redundancy in different layers. In this work, we investigate a simple-yet-effective method for pruning channels based on a computationally lightweight yet effective data driven optimization step that discovers the necessary width per layer. Experiments conducted on ILSVRC-12 confirm effectiveness of our approach. With non-uniform pruning across the layers on ResNet-50, we are able to match the FLOP reduction of state-of-the-art channel pruning results while achieving a 0.98% higher accuracy. Further, we show that our pruned ResNet-50 network outperforms ResNet-34 and ResNet-18 networks, and that our pruned ResNet-101 outperforms ResNet-50.

1 Introduction

In recent years, convolutional neural networks (CNNs) have become the predominant approach for a variety of computer vision tasks, e.g. image classification [18], object detection [5], semantic segmentation [24], image captioning [32], and video analysis [28]. Supported by the availability of high end modern GPUs and large scale

labeled data sets [4], the state-of-the-art CNN architectures have grown unprecedentedly large. For instance, a 152-layer ResNet [11] comprises more than 60 million parameters and requires more than 20 Giga floating-point-operations (FLOPs) when inferring an image of 224×224 resolution.

Such large networks admit large inference latency and require more space in memory. Therefore, Most of the standard CNN architectures have smaller versions. For example, ResNet has five standard sizes: ResNet-152, ResNet-101, ResNet-50, ResNet-34, and ResNet-18, where X in ResNet- X represent the number of convolutional layers. Similarly, MobileNet has three three standard sizes: MobileNet-1.0, MobileNet-0.5, MobileNet-0.25. All the three versions have the same number of convolutional layers, however uniformly across all the layers the number of filters in MobileNet-0.5 is half that of the MobileNet-1.0.

In this work, we ask the following question: can we get an architecture more efficient than ResNet-34 by pruning channels of ResNet-50? In generality, can we get architectures more efficient than the expert-designed smaller versions of a large network by pruning channels of the large network in a data-driven way? By efficient architecture we mean an architecture which is better in terms of accuracy or latency/throughput/#FLOPS/#params. To the best of our knowledge none of the existing channel pruning works compare the pruned versions of a large network with the next available standard smaller network, for large data-sets like ImageNet.

The recent works on model compression can be divided into four main categories, namely, quantization [3, 27, 15], low rank factorization [16, 20, 31], sparse connections [7, 8], and structured sparsity such as channel pruning [33, 25, 23, 35]. Network quantization aims to reduce the model size and accelerate the inference by reducing precision of the network weights. Many of the modern computing devices support faster infer-

ence for the low precision networks. Low rank factorization approximates the convolutional kernels using tensor decomposition techniques. Sparse connections seeks to sparsify the network by pruning low importance weights in the model. We note that unstructured sparsity may lead to a reduction in the number of parameters, but typically will not accelerate the network due to its inherent need to access memory in a non-consecutive way. In contrast, channel pruned network has exactly the same architecture and back-end implementation but with fewer filters and channels. Hence it immediately yields smaller memory footprint and faster inference than the original model without requiring any additional hardware or software support. Further, channel pruning is complementary to network quantization and it is known that both can be applied together to achieve higher compression than any method individually [7].

2 Summary of Results

In this work, we aim to investigate simple yet effective methods to perform channel pruning in the entire network across the layers, allowing the possibility of pruning more channels in one layer compared to others. This freedom gives our results a flavor of architecture search, as the resulting model’s architecture is based on the dataset rather than an educated guess. We compare the pruned ResNet models with the next available standard smaller model. Figure 1 shows a scatter plot of various models. The x-axis represents throughput and the y-axis corresponds to accuracy. The grey colored dots represent our PruneNets, the networks obtained by pruning channels of ResNet-50. The base models and their training script have been taken from MXNET GluonCV GitHub repository. It can be seen that the PruneNets (pruned ResNet-50) significantly outperform ResNet-34, ResNet-18 and MobileNet-1.0. Pruned ResNet-101 (light pink color) outperforms ResNet-50 (black color). The light blue color dot on the extreme right represents pruned ResNet-34. The pruned ResNet models are available in GluonCV repository and their performance can be seen on accuracy-vs-throughput plot on its webpage https://gluon-cv.mxnet.io/model_zoo/classification.html.

In Figure 1, we have pruned channels to maximize throughput on a batch-size of 64 for NVIDIA V100 GPU. However, in general the objective of pruning channels can vary. We may want to minimize #FLOPs or memory footprint or maximize throughput for a different

batch-size on a different CPU/GPU machine. Our channel pruning approach takes the particular objective into consideration and accordingly gives different pruning pattern across the layers.

Figure 2 and Figure 3 show the channel pruning patterns achieved by our approach when the objective is to minimize #FLOPs ($3.47\times$ reduction) and when the objective is to minimize the number of parameters ($2.95\times$ reduction) respectively. When the objective is to minimize the #FLOPs, Figure 2, the layers closer to the input are pruned aggressively whereas when the objective is to minimize the #Params, Figure 3, the layers closer to the output are pruned heavily. This very different pruning pattern depending upon the pruning objective can be understood by the fact that the layers closer to the input are more compute intensive (size of feature map is larger in the layers closer to the input) whereas the layers closer to the output are more parameter intensive (number of channels is larger in the layers closer to the output). The accuracy of these pruned networks are given in the eleventh row of Table 3 and the seventh row of Table 4 respectively in Section 5.

We note that most of the existing channel pruning works uniformly prune the channels across all the layers, or minimize the number of channels in the network ignoring the real objective (reducing FLOPs/Params) of channel pruning.

In Section 4 we explain our channel pruning approach in detail. In Section 5 we provide experiments on several ResNet architectures, on the ILSVRC-12 (ImageNet) dataset. Since the existing channel pruning works only report reduction in memory footprint and FLOPs count, for comparison purpose we restrict to these two objectives. The resulting PruneNets achieve state-of-the-art performance when compared to other pruned models reported in the literature. In order to test the resulting model we assess not only its performance on a test set, but its applicability in other tasks. We use a common transfer learning task and measure how a pruned ResNet-50 model performs when fine tuned on the Caltech-256 dataset. The performance of the pruned model is comparable and in some settings even better than that of the original ResNet-50 model.

3 Related works

There have been a significant amount of work on compressing and accelerating deep CNNs. Most of these works fall primarily into one of the four categories: quan-

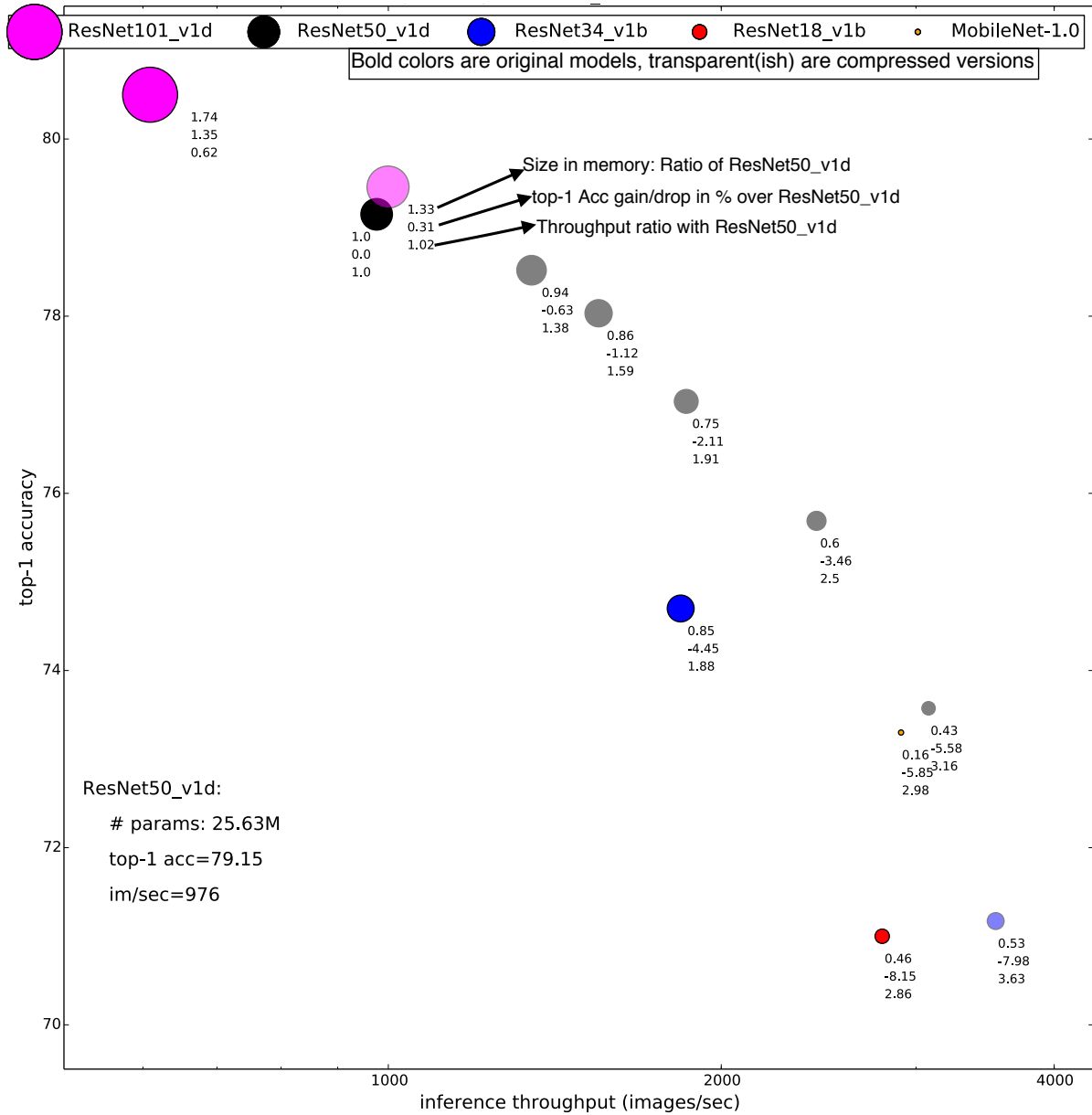


Figure 1: The black circle corresponds to ResNet-50 model. It has 25.63 million parameters, 79.15% top-1 accuracy on ImageNet dataset, and it gives a throughput of 1060 images/sec for batch size of 64 on a NVIDIA V100 GPU. The other colored circles represent the other state-of-the-art models. The grey circles represent our PruneNets. The three numbers associated with each of these circles show the following: the first number gives size of the model (multiplicative w.r.t. ResNet-50), the second number gives loss in accuracy w.r.t. ResNet-50, and the third number gives multiplicative gain in throughput w.r.t. ResNet-50.

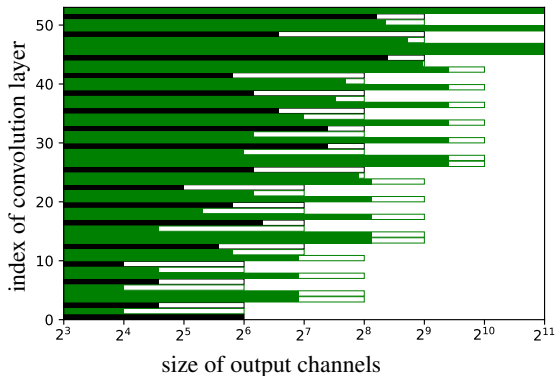


Figure 2: Pruning pattern achieved by our approach when the objective is to minimize #FLOPs. Shallow layers are pruned aggressively. The black bars represent 3×3 convolution layers and the green bars represent 1×1 convolution layers. The white colored area in each bar represents pruning.

tization, low rank factorization, sparse connections, and structured pruning. Besides compression methods, there have been a lot of work in architecture search for compute efficient networks [22, 29]. Recently, model compression techniques has also been applied on natural language processing models [19, 17].

Quantization approaches do not reduce the number of parameters but rather their precision, meaning the number of bits representing each parameters. This is done by quantizing the parameters to binary [27, 15], ternary [34], or 4 or 8 bits per parameter [7, 6]. Low rank factorization techniques exploit various low rank structures in the convolution parameters, such as a basis for the filters [16], or a tensor low rank decomposition [20, 31]. We note that the practical compression and the acceleration achieved with these low-rank approaches is currently limited as the standard deep learning libraries do not support convolutional operation by low rank weight tensors.

Different methods have been explored to prune the model parameters. The early work by [9] performed magnitude based pruning and [10] suggested Hessian matrix based approach to prune the network weights. More recently, [8] introduced an iterative method to prune weights in deep architectures, together with an external compression by quantization and Huffman encoding [7]. The network is pruned by removing low weight connections, followed by fine-tuning to recover its accuracy. Training with sparsity constraints has also been studied by [30, 33] to achieve higher compression.

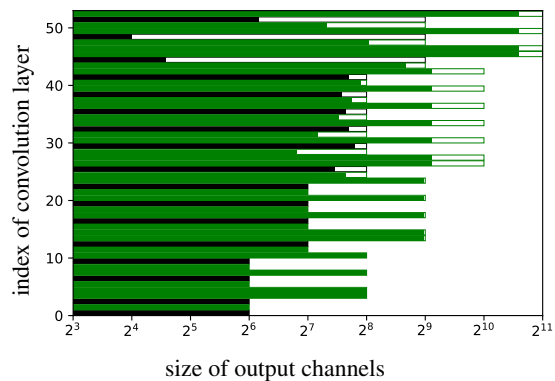


Figure 3: Pruning pattern achieved by our approach when the objective is to minimize #Params. Deep layers are pruned aggressively. The black bars represent 3×3 convolution layers and the green bars represent 1×1 convolution layers. The white colored area in each bar represents pruning.

[14] extends parameter pruning and seeks to identify the optimal number of parameters that should be pruned in each layer to minimize the loss in accuracy for a given budget on the pruning. They achieve this by using a measure of average percentage of zeros (APoZ) for each layer.

Existing works in channel pruning can be divided into two categories: training from scratch and pruning redundant channels in a pretrained network. The first type [33, 1, 23] trains the network with regularization terms aimed to induce sparsity along the channels. This approach has several shortcomings. First, by requiring full training it does not apply to situations where we already have a trained model and we aim to compress it in a lighter procedure involving either less computation or less data. Second, the sparsity inducing regularization can often insert bias that degrades performance. This issue can be somewhat mitigated by considering non-convex regularization or some iterative pruning approach (see e.g. [2]); this fix however comes at the expense of a complicated system that requires a longer training time due to new hyper parameters to be optimized, or the need for multiple training rounds when pruning repeatedly without sparsity inducing regularization. Non-convex regularization typically has more than one parameter associated with it, informally determining how far away it is from L1 regularization. Another issue comes up in networks that use Batch Norm [23]. In all recent architectures a batch-norm layer is present after every convolution. The normalization operation done by this

layer can completely modify the effect of a regularization term, as the magnitude of the parameters does not change the output of the model. For example, [13] show that the ℓ_2 regularization term’s effect can be mimicked with a learning rate schedule, meaning that the ‘weight-decay’ parameter helps more as a learning rate scheduler as opposed to a regularization parameter. This result along with additional papers cited within suggest that a naive combination of sparsity inducing regularization combined with batch-norm may not have the desired effect.

The second type of channel pruning works that start with a pretrained model can be further sub-categorized into two. First sub-category of works prune channels uniformly in each layer using reconstruction based approaches [25, 12]. The high level mode of operation is to obtain a sample of inputs and outputs of a convolutional layer, then learn a layer with lesser input channels that produce approximately the same output. The measure of approximation is typically in ℓ_2 norm but can be more sophisticated, see e.g. [35]. The main drawback of these methods comes from the fact they handle convolutional layers one at a time. As such, they cannot detect correlations occurring across layers, and more important, it is hard to adapt these methods to prune one layer more aggressively than another. It follows that these works are inherently limited as they prune the same fraction of channels across all the layers. Our methods can in fact be seen as complimentary to these results, as we provide a light-weight scheme that among others, discovers the extent by which the layers should be pruned. The second sub-category of works prune channels in a pretrained model based on the network parameters and their basic statistics. [21] prunes channels based on the ℓ_1 norm of the filters, and [14] defines redundancy of neurons based on their activations and prunes the more redundant ones. In contrast to these methods, our method is optimization driven. Instead of identifying redundancy of channels based on parameter values of the pretrained model we optimize over parameters which correlate with the redundancy of the channels. Therefore our method encompasses these existing methods and improves upon them.

Our paper presents a channel pruning technique that enjoys the global view and precise pruning of the full training techniques, while requiring a short training time for the pruning procedure, similarly to the techniques that prune based on basic statistics of the weights. In contrast to the papers described above, the importance of channels is based on the motivating example of sparse

linear regression, takes into account the affects of Batch-Norm, and most importantly, is based on a short (handful of epochs) training procedure rather than the model weights or a few basic statistics of the data. Our claim that this technique achieves a more accurate importance ranking for the channels is backed up by our experiments achieving state-of-the-art results on ResNet architectures on the ImageNet dataset.

4 Approach

We begin by formally characterizing a CNN and its parameters. For readability we assume the structure of Convolution-BatchNorm-Activation and a ReLU activation. We note that our framework applies without this assumption, meaning for any order and for any activation type. Let L denote the number of convolution operators in the network, and for $\ell \in [L] = \{1, \dots, L\}$ let $W_\ell \in \mathbb{R}^{n_\ell \times m_\ell \times k_\ell \times k_\ell}$ denote the filter weights of the ℓ -th convolution. Here, n_ℓ and m_ℓ represent the number of output and input channels respectively, and $k_\ell \times k_\ell$ is the size of each filter. A BatchNorm (BN) layer has the same input and output size. Denote by $z^{(in)} \in \mathbb{R}^{n \times r \times r}$ and $z^{(out)} \in \mathbb{R}^{n \times r \times r}$ its input and output respectively. Here, the z variables contain n channels, each assumed to have $r \times r$ features. This assumption is purely for readability. Our framework works for 1d or 3d convolution as well, with any feature map size. Let \mathcal{B} denote the current mini-batch, a standard BN layer performs the following affine transformation for each i -th feature map $z_i \in \mathbb{R}^{r \times r}$, for $i \in \{1, 2, \dots, n\}$.

$$\hat{z}_i = \frac{z_i^{(in)} - \mu_{\mathcal{B}_i}}{\sqrt{\sigma_{\mathcal{B}_i}^2 + \epsilon}}; \quad z_i^{(out)} = \gamma_i \hat{z}_i + \beta_i, \quad (1)$$

where $\mu_{\mathcal{B}_i}$ is the scalar mean of the entire i -th feature map over the mini-batch \mathcal{B} , and $\sigma_{\mathcal{B}_i}^2$ is the scalar variance. Although individual numbers within the feature map \hat{z}_i do not have a zero mean and unit variance, each feature map \hat{z}_i , when considered as a r^2 -dimensional vector, has unit norm and sums to zero, in expectation. With this in mind, we say that γ_i^2 controls the variance of the i -th output channel $z_i^{(out)}$, and β_i is its mean.

When doing inference, the BN layer behaves slightly differently. Rather than taking the mini-batch statistics ($\mu_{\mathcal{B}_i}, \sigma_{\mathcal{B}_i}^2$), it uses their global counterparts (μ, σ^2) obtained not from a single mini-batch but from the entire dataset (or sufficiently large sample). Since each convolution is followed by a BN layer, we let $\gamma_{\ell, i}, \beta_{\ell, i}$

represent the i -th scale and bias parameters of the ℓ -th convolution layer.

For the entire network, let $W \equiv \{W_\ell\}_{\{1,2,\dots,L\}}$ denote the set of all convolution parameters, and let $\gamma = \{\gamma_{\ell,i}, \beta_{\ell,i}\}_{\ell,i}$ denote the parameters of the BN layers following the convolutions. Denote all other network parameters by F . This could include fully connected layers etc.

4.1 Global Importance Score

We are now ready to explain our approach and the motivation leading to it. We first observe that if we ignore the effect of the activations, the i -th input channel of the ℓ -th convolution layer has a variance of $\gamma_{\ell-1,i}^2$. Therefore, the contribution of the i -th input to the variance of the j -th output in the ℓ -th convolution layer is

$$\gamma_{\ell-1,i}^2 \|W_{\ell,i,j}\|_2^2, \quad (2)$$

where $W_{\ell,i,j}$ is the filter in the ℓ -th convolution layer corresponding to the i -th input and the j -th output. Indeed if the filters and input feature maps were of dimension 1, then the convolution would be reduced to a linear function. In this simplified case where the convolution is reduced to a linear function, if we wanted to ignore one of the inputs and minimize the squared distance of the output change for the j -th output channel, the importance of the inputs would exactly be determined by the importance score in Equation (2). When considering all outputs simultaneously the score becomes

$$\gamma_{\ell-1,i}^2 \sum_{j=1}^{n_\ell} \|W_{\ell,i,j}\|_2^2. \quad (3)$$

We let this score be the global importance score of the i -th input channel to the ℓ -th convolution layer. Now, since the ReLU activation is linear, and as detailed before, when applying sparsity regularization we do not modify the convolution weights W , rather we multiply the convolution weights with a scalar such that $\sum_{j=1}^{n_\ell} \|W_{\ell,i,j}\|_2^2 = 1$ and shift that scalar into $\gamma_{\ell-1,i}$ and $\beta_{\ell-1,i}$. For this reason, when we discuss the details of our implementation we will assume that the importance score is simply $\gamma_{\ell-1,i}$.

4.2 Regularization and Importance Scores

Given this Global Importance Score, a naive approach for pruning channels of a pretrained network would be

to rank all the channels according to their score and prune the least important ones. However, a sophisticated approach would be to train a model while regularizing the cost associated with each channel and then prune the low importance channels.

Let's proceed to define our optimization objective. First, denote by

$$\mathcal{L}\left(f(x; \{W, F, \gamma, \beta\}; \{\mu_B, \sigma_B^2\}), y\right), \quad (4)$$

the loss of the network during a standard training. The most straightforward objective when considering channel pruning is

$$(4) + \lambda \sum_{\ell > 1, i} \alpha_\ell \mathbf{1}[\gamma_{\ell-1,i} > 0]$$

Here, a channel with $\gamma_{\ell,i} = 0$ is considered pruned even if $\beta_{\ell,i} \neq 0$, since the bias term can be simulated by modifying the other network parameters. We let α_ℓ denote the cost associated with each input channel of the ℓ -th convolutional layer. The value of the α costs are determined by our objective. For example, for FLOPs minimization we compute the number of FLOPs needed for the full network, and for the network after pruning an output of the $(\ell - 1)$ -th layer which is also an input to the ℓ -th layer. This difference determines the scale of α_ℓ . The objective of channel pruning can be any of the following: minimize the model size (# params), reduce the # FLOPs required for inferencing an image, or minimize latency on a given hardware (GPU/CPU). We choose the costs α_ℓ according to the objective.

Since ℓ_0 norm is non-smooth and has zero gradient almost everywhere, we consider the standard continuous relaxation of it and use the ℓ_1 norm which is well known to induce sparsity. Therefore, we seek to minimize the following objective function. We note that there are papers that use various non-convex regularization. We postpone exploring the benefit of those to future works, so as to minimize the number of unknowns.

$$\mathcal{L}\left(f(x; \{W, F, \gamma, \beta\}; \{\mu_B, \sigma_B^2\}), y\right) + \lambda \sum_{\ell,i} \alpha_\ell |\gamma_{\ell,i}|. \quad (5)$$

4.3 Optimize with BatchNorm off

An immediate approach would be to optimize the regularized objective in (5) by training all the model parameters W, F, γ, β with random initialization. Recall (μ_B, σ_B^2)

are the mini-batch mean and variance values, not the trainable model parameters. However, a closer investigation of BatchNorm layer, (1), reveals that in doing so the impact of regularizing $\gamma_{\ell,i}$ would be nullified by the normalization operation in the BatchNorm layer. Particularly, the regularization term $\sum_{\ell,i} \alpha_{\ell} |\gamma_{\ell,i}|$ can be pushed to any arbitrary positive value $\epsilon > 0$ without changing the network output and the loss function $\mathcal{L}(\cdot)$. It can be seen that for any given scalar $\tau > 0$ there exists $\tilde{\gamma} = \tau\gamma$, $\tilde{\beta} = \tau\beta$, $\tilde{\mu}_B = \tau\mu_B$, and $\tilde{\sigma}_B^2 = \tau^2\sigma_B^2$, such that

$$\begin{aligned} & \mathcal{L}\left(f(x; \{W, F, \gamma, \beta\}; \{\mu_B, \sigma_B^2\}), y\right) \\ = & \mathcal{L}\left(f(x; \{W, F, \tilde{\gamma}, \tilde{\beta}\}; \{\tilde{\mu}_B, \tilde{\sigma}_B^2\}), y\right). \end{aligned}$$

Note that when the γ and β are reduced by a factor of τ then by definition, (1), the mean and variance of feature maps change to $\tilde{\mu}_B$ and $\tilde{\sigma}_B^2$. Therefore, we propose optimizing the regularized objective (5) by turning the BatchNorm layer off. We do so by fixing the BatchNorm mean and variance values (μ_B, σ_B^2) to their global counterparts (μ, σ^2) . Note that during inference also (μ_B, σ_B^2) are set to (μ, σ^2) . Further, the convolutional weight parameters W also have the same impact on the regularization term; γ and β can be reduced by a factor of τ while keeping the network output same by increasing W by a factor of $1/\tau$. Therefore, we start with a pretrained model and fix the convolution weight parameters W to their value W^* in the pre-trained network. We minimize the following objective to induce sparsity in γ .

$$\begin{aligned} & \mathcal{L}\left(f_{(W^*, \mu, \sigma^2)}(x; \{F, \gamma, \beta\};), y\right) \\ & + \lambda \sum_{\ell,i} \alpha_{\ell} |\gamma_{\ell,i}|. \end{aligned} \quad (6)$$

Note that the objective is only a function of BatchNorm scale parameters γ, β and the fully connected layer parameters F . Since F is typically a single fully connected layer, the overall number of parameters to be optimized is small and a single epoch suffices.

Note that [23] follows the approach of optimizing the objective in (5) by training all the model parameters W, F, γ, β with random initialization. However, as explained above this approach nullifies the effect of regularizing γ , and requires a long time to converge due to the large number of parameters in W .

4.4 Step-wise Pruning of Channels

The step of optimizing (6) leaves us with a ranking of the channels based on their Importance Score γ . We

prune sufficiently many channels to reduce the total cost $C = \sum_{\ell,i} \alpha_{\ell}$ to ηC , for a given fraction η . By prune we mean we set their γ value to zero if it wasn't already zero, and move on to the next phase.

In the next phase we fix the bias suffered by the sparsity inducing regularization and optimize

$$\mathcal{L}\left(f_{W^*}(x; \{F, \gamma, \beta\}; \{\mu_B, \sigma_B^2\}), y\right), \quad (7)$$

the same objective as in (6) but without the regularization term. In this step, we use the mini-batch mean and variance values (μ_B, σ_B^2) for BatchNorm layers. Also, we compute the updated values of their global counterparts (μ, σ) which are used in the next iteration of the regularization, (6). Here, we abused notation and use γ to denote the set of non-pruned weights. The pruned weights are fixed as zeros. As before, since the number of parameters here is small, a single epoch typically suffices to solve the optimization problem.

Finally, we alternately repeat optimizing objectives (6) and (7) for T times. In each step we reduce the cost by $(\eta/T)C$ for a desired fraction of cost reduction η . We optimize the hyper-parameters associated with these two steps in a way that minimizes the loss of Equation (7). Since the overall procedure is lightweight, exploring hyper-parameters is much cheaper compared to those relevant to a full training job.

Once we obtained the final pruned model, we fine tune all of its weights, including W , by optimizing objective (4), with the appropriate γ values being fixed as zeros. The following Algorithm 1 summarizes our approach.

5 Experiments

In this section, we empirically evaluate the performance of our Global Channel Pruning (GCP) algorithm. The GCP operates on a pretrained model and requires two inputs: the minimization objective, for e.g. minimize # FLOPs, and the target fraction, η . The target fraction η is the ratio of the desired objective value in the pruned network and the objective value in the original network. Note that we chose the regularization scale α_{ℓ} for each channel $\ell \in \{1, 2, \dots, L\}$ according to the objective we seek to minimize. We refer GCP by GCP-p when α_{ℓ} are chosen to minimize the # params and by GCP-f when α_{ℓ} are chosen to minimize # FLOPs. We refer GCP by GCP- ℓ when α_{ℓ} are chosen to minimize the latency. Our

Algorithm 1 Global Channel Pruning (GCP)

Input: A CNN architecture, Minimization objective (# FLOPs/ # Params), target fraction η , T : number of iterations.

Output: A pruned CNN model.

Train the network using loss (4).

Let W^* be the filter weights of the trained network.

Repeat T times:

Fix W^* and the BN mean and variance parameters to their global counterparts.

Train the network with regularization on γ 's using loss (6).

Rank the channels according to their global importance score γ .

Prune channels according to their importance score to achieve η/T reduction in the target objective value (# FLOPs/ # Params)

Train the network without regularization term on γ using loss (7)

Retrain the pruned network including filter weights W^* using loss (4).

method can also be used to maximize throughput as it is the inverse of latency.

We evaluate GCP on state-of-the-art ResNet models for ILSVRC-12 (ImageNet) and Caltech-256 datasets. We compare performance of GCP against several well known channel pruning methods, including Discrimination Aware Channel Pruning (DCP) [35], ThiNet[25], and Channel Pruning (CP) [12]. To the best of our knowledge, these are the state-of-the-art works that report channel pruning results on ResNet models for ImageNet dataset. These works set a target fraction η for pruning channels and uniformly prune the η fraction of channels from each layer. However, since the true objective of channel pruning is to reduce the # params and # FLOPs, they report these numbers as well. To fairly compare with these works we run GCP-f with the target fraction η equal to the FLOPs reduction reported in these works, and run GCP-p with η set to the parameter reduction reported in these works.

Besides, to investigate the effect of the non-uniform pruning achieved by GCP, we study the uniform pruning approach wherein we prune each layer uniformly. We prune η fraction of channels from each layer in the pre-trained model and retrain the pruned model. Though the DCP/ThiNet/CP prune uniformly across the layers, they are significantly distinct than the naive uniform pruning approach. They employ variants of reconstruction based

approaches to identify which channels to prune in the each layer as against randomly pruning η fraction of channels.

5.1 Implementation details

We implement GCP on the MXNET deep learning framework. For training the original ResNet networks, we use the training script provided in the MXNET library- GluonCV.

ResNet is a residual network architecture. It has many skip connections which require that the size of the output channels be same for the layers connected by the skip connections. If the size of the output channels is not same, then it requires sparse additions in the residual addition layer instead of the standard element-wise addition. Since the standard deep learning libraries, including MXNET, are highly optimized to perform the standard convolution operations faster, such sparse addition layers tend to slow down the network. Therefore, we restrict the pruning of layers connected by the skip connection to be identical. This is done by multiplying (element-wise) a mask parameter $\tilde{\gamma}_a$ to all the γ_ℓ parameters of the layers which need to be pruned identically (due to the dependency enforced by the skip connection). Instead of regularizing γ_ℓ 's for these layers we regularize $\tilde{\gamma}_a$, which ensures that these layers are pruned identically. Further, we use proximal gradient descent [26] to optimize the γ parameters during the regularization step when we need to sparsify γ .

5.2 Comparisons on ILSVRC-12

ILSVRC-12 (ImageNet) contains 1.28 million training images and 50 thousand testing images for 1000 classes. This is one of the most widely used datasets for evaluating performance of CNNs. Further, networks trained on ImageNet are commonly used for transfer learning on smaller datasets such as Caltech-256. We show effectiveness of GCP on three different ResNet architectures, namely ResNet-18, ResNet-50 and ResNet-101. On all the three networks, in the high pruning regime, GCP outperforms the baselines models with a significant margin. In the low pruning regime, its performance is comparable to the baseline models. In all the settings, it performs better than the naive uniform pruning.

ResNet-18	# Params. ↓	# FLOPs ↓	Top-1	Top-5
DCP	1.39×	1.37×	+0.43	+0.12
Uniform	1.42×	1.35×	+1.31	+0.67
GCP-f	1.03×	1.36×	+0.45	+0.32
DCP	1.89×	1.85×	+2.29	+1.38
Uniform	1.92×	1.85×	+3.01	+1.90
GCP-f	1.19×	1.87×	+1.70	+1.06
DCP	2.92×	2.79×	+5.52	+3.30
Uniform	2.76×	2.79×	+6.75	+4.2
GCP-f	1.53×	2.81×	+4.34	+2.70

Table 1: Comparisons on ILSVRC-12 for ResNet-18. The top-1 and top-5 error % of the pre-trained model are 29.21 and 10.13 respectively. The proposed method GCP-f incurs 1.18% lower error rate than the DCP method for the same $2.81\times$ reduction in # FLOPs.

5.2.1 Resnet-18

Table 1 gives the results of channel pruning of ResNet-18 for various FLOPs reduction targets. For example, the numbers in the sixth row correspond to the results of GCP-f for # FLOPs minimization with target fraction $\eta = 1/1.87$. It returns a pruned model that has $1/1.19$ fewer parameters, 1.70% higher top-1 and 1.06% higher top-5 error rate than the original pretrained model. Compared to this, DCP achieves the same # FLOPs reduction at 2.29% increase in top-1 error rate. Note that since GCP-f prunes channels non-uniformly, its parameter reduction is not same as its FLOPs reduction unlike the case of naive Uniform pruning and the DCP approach which prunes channels uniformly.

Table 2 gives similar results for the case of GCP-p applied on ResNet-18 for minimizing the model parameters. Again, in the high pruning regime, GCP-p significantly outperforms the DCP [35].

5.2.2 ResNet-50

Table 3 gives the results of channel pruning of ResNet-50 for various FLOPs reduction targets. For example, the numbers in the eleventh row correspond to the results of GCP-f for # FLOPs minimization with target fraction $\eta = 1/3.47$. It returns a pruned model that has $1/2.18$ fewer parameters, 2.28% higher top-1 and 1.35% higher top-5 error rate than the original pretrained model. Compared to this, DCP achieves the same # FLOPs reduction at 3.26% increase in top-1 error rate. Further, the last four rows show the gain of GCP-f over uniform pruning

ResNet-18	# Params. ↓	# FLOPs ↓	Top-1	Top-5
DCP	1.39×	1.37×	+0.43	+0.12
GCP-p	1.41×	1.09×	+0.71	+0.31
DCP	1.89×	1.85×	+2.29	+1.38
GCP-p	1.89×	1.21×	+1.84	+1.18
DCP	2.92×	2.79×	+5.52	+3.30
GCP-p	2.97×	1.38×	+5.21	+2.84

Table 2: Comparisons on ILSVRC-12 for ResNet-18. The top-1 and top-5 error % of the pre-trained model are 29.21 and 10.13 respectively. In the high pruning regime, the proposed method GCP-p outperforms the DCP.

in the extreme setting of $5\times$ and $10\times$ FLOPs reduction.

Table 4 gives similar results for the case of GCP-p applied on ResNet-50 for minimizing the model parameters. Again, in the high pruning regime, GCP-p significantly outperforms the DCP [35].

Figure 1 in Section 2 shows the results of GCP- ℓ applied on ResNet-50 for maximizing the throughput for a batch-size of 64 on a NVIDIA V100 GPU. As discussed in Section 2, PruneNets significantly outperform the smaller networks- ResNets-34, ResNet-18 and MobileNet 1.0.

5.2.3 ResNet-101

Table 5 gives the results of channel pruning of ResNet-101 network for various FLOPs reduction targets. For both the FLOPs reduction target values of $\eta = 1/2$ and $\eta = 1/3.35$, GCP-f outperforms the naive uniform pruning approach. Figure 1 in Section 2 shows the results of GCP- ℓ applied on ResNet-101 for maximizing the throughput for a batch-size of 64 on a NVIDIA V100 GPU, and results in a network both faster and more accurate than ResNet-50.

5.3 Comparisons on Caltech-256

In the following we show that the pruned ResNet models when used for transfer learning on smaller dataset such as Caltech-256 performs comparable to the original model. Caltech-256 contains 30 thousand images for 256 classes. We resize the top fully connected layer of the pruned ResNet network to match the output size of 256 classes and randomly initialize its weights. For training and testing we follow the standard protocol. We sample 60 images from each class as the training set,

ResNet-50	# Params. ↓	# FLOPs ↓	Top-1	Top-5
DCP	1.51×	1.56×	-0.39	-0.14
Uniform	1.57×	1.55×	+0.57	+0.18
GCP-f	1.12×	1.55×	+0.38	+0.17
ThiNet	2.06×	2.25×	+1.87	+1.12
DCP	2.06×	2.25×	+1.06	+0.61
CP	-	2×	-	+1.40
Uniform	2.26×	2.24×	+1.37	+0.74
GCP-f	1.32×	2.24×	+1.02	+0.56
DCP	2.94×	3.47×	+3.26	+1.80
Uniform	3.51×	3.46×	+3.10	+2.14
GCP-f	2.18×	3.47×	+2.28	+1.35
Uniform	5×	5×	+5.08	+2.8
GCP-f	3.09×	5×	+3.86	+2.06
Uniform	10×	10×	+10.05	+5.89
GCP-f	5.75×	10×	+8.16	+4.89

Table 3: Comparisons on ILSVRC-12 for ResNet-50. The top-1 and top-5 error % of the pre-trained model are 22.81 and 6.47 respectively. “-” denotes that the results are not reported.

ResNet-50	# Params. ↓	# FLOPs ↓	Top-1	Top-5
DCP	1.51×	1.56×	-0.39	-0.14
GCP-p	1.51×	1.13×	-0.05	-0.19
ThiNet	2.06×	2.25×	+1.87	+1.12
DCP	2.06×	2.25×	+1.06	+0.61
GCP-p	2.08×	1.32×	+0.55	+0.20
DCP	2.94×	3.47×	+3.26	+1.80
GCP-p	2.95×	1.53×	+1.52	+0.65

Table 4: Comparisons on ILSVRC-12 for ResNet-50. The top-1 and top-5 error % of the pre-trained model are 22.81 and 6.47 respectively.

ResNet-101	# Params. ↓	# FLOPs ↓	Top-1	Top-5
Uniform	2.03×	2×	+0.95	+0.34
GCP-f	1.56×	2×	+0.68	+0.18
Uniform	3.59×	3.35×	+2.35	+0.75
GCP-f	2.12×	3.35×	+2.11	+0.54

Table 5: Comparisons on ILSVRC-12 for ResNet-101. The top-1 and top-5 error % of the pre-trained model are 19.57 and 4.94 respectively.

ResNet-50	# Params. ↓	# FLOPs ↓	Top-1	Top-5
GCP-f	1.12×	1.55×	-0.78	-0.31
GCP-f	1.32×	2.24×	+0.16	+0.03
GCP-f	2.18×	3.47×	+0.98	+0.23
GCP-f	3.09×	5×	+2.18	+0.67
GCP-f	5.75×	10×	+7.53	+3.87

Table 6: Comparisons on Caltech-256 for ResNet-50. The top-1 and top-5 error % of the pre-trained model are 18.96 and 9.73 respectively.

and the rest for the test set. We fine-tune the network for 60 epoch with a learning rate of 0.01 with cosine learning scheduler. Table 6 compares the results obtained from various pruned versions of ResNet-50 with those obtained via the unpruned ResNet-50. For the lightest pruned version of ResNet-50 (1.55× FLOPs reduction), the performance actually improved. It remains comparable even with 2.24× FLOPs reduction.

6 Discussion

We note that our choice of DCP [35] as the main baseline is due to the fact that they achieve the state-of-the-art results of compressing ResNet50 on ImageNet via channel pruning, and not due to our method being an alternative to theirs. We in fact view our method as complementary the theirs in that it provides a clean way to learn the required width of each layer. It is in fact reasonable to assume that the specialized manner in which they optimize the weights of their network is advantageous compared to ours and that accounts for their superiority in the regime of mild pruning. However, once we require a more aggressive pruning, our method is superior due to increased gain from non-uniform pruning. An interesting follow up would be a method combining the techniques, using our methods for attaining the architecture, combined with alternative methods for tuning the weights of the new network.

References

- [1] Jose M Alvarez and Mathieu Salzmann. Learning the number of neurons in deep networks. In *Advances in Neural Information Processing Systems*, pages 2270–2278, 2016.
- [2] Miguel A Carreira-Perpinán and Yerlan Idelbayev. learning-compression algorithms for neural net pruning.

- In *Proceedings of the IEEE Conference on Computer Vision and Pattern Recognition*, pages 8532–8541, 2018.
- [3] Matthieu Courbariaux, Yoshua Bengio, and Jean-Pierre David. Binaryconnect: Training deep neural networks with binary weights during propagations. In *Advances in neural information processing systems*, pages 3123–3131, 2015.
- [4] Jia Deng, Wei Dong, Richard Socher, Li-Jia Li, Kai Li, and Li Fei-Fei. Imagenet: A large-scale hierarchical image database. In *Computer Vision and Pattern Recognition, 2009. CVPR 2009. IEEE Conference on*, pages 248–255. Ieee, 2009.
- [5] Ross Girshick, Jeff Donahue, Trevor Darrell, and Jitendra Malik. Rich feature hierarchies for accurate object detection and semantic segmentation. In *Proceedings of the IEEE conference on computer vision and pattern recognition*, pages 580–587, 2014.
- [6] Yunchao Gong, Liu Liu, Ming Yang, and Lubomir Bourdev. Compressing deep convolutional networks using vector quantization. *arXiv preprint arXiv:1412.6115*, 2014.
- [7] Song Han, Huizi Mao, and William J Dally. Deep compression: Compressing deep neural networks with pruning, trained quantization and huffman coding. *arXiv preprint arXiv:1510.00149*, 2015.
- [8] Song Han, Jeff Pool, John Tran, and William Dally. Learning both weights and connections for efficient neural network. In *Advances in neural information processing systems*, pages 1135–1143, 2015.
- [9] Stephen José Hanson and Lorien Y Pratt. Comparing biases for minimal network construction with back-propagation. In *Advances in neural information processing systems*, pages 177–185, 1989.
- [10] Babak Hassibi and David G Stork. Second order derivatives for network pruning: Optimal brain surgeon. In *Advances in neural information processing systems*, pages 164–171, 1993.
- [11] Kaiming He, Xiangyu Zhang, Shaoqing Ren, and Jian Sun. Deep residual learning for image recognition. In *Proceedings of the IEEE conference on computer vision and pattern recognition*, pages 770–778, 2016.
- [12] Yihui He, Xiangyu Zhang, and Jian Sun. Channel pruning for accelerating very deep neural networks. In *International Conference on Computer Vision (ICCV)*, volume 2, 2017.
- [13] Elad Hoffer, Ron Banner, Itay Golan, and Daniel Soudry. Norm matters: efficient and accurate normalization schemes in deep networks. In *NeurIPS*, pages 2164–2174, 2018.
- [14] Hengyuan Hu, Rui Peng, Yu-Wing Tai, and Chi-Keung Tang. Network trimming: A data-driven neuron pruning approach towards efficient deep architectures. *arXiv preprint arXiv:1607.03250*, 2016.
- [15] Itay Hubara, Matthieu Courbariaux, Daniel Soudry, Ran El-Yaniv, and Yoshua Bengio. Quantized neural networks: Training neural networks with low precision weights and activations. *Journal of Machine Learning Research*, 18(187):1–30, 2017.
- [16] Max Jaderberg, Andrea Vedaldi, and Andrew Zisserman. Speeding up convolutional neural networks with low rank expansions. *arXiv preprint arXiv:1405.3866*, 2014.
- [17] Ashish Kheta and Zohar Karnin. schubert: Optimizing elements of bert. *arXiv preprint arXiv:2005.06628*, 2020.
- [18] Alex Krizhevsky, Ilya Sutskever, and Geoffrey E Hinton. Imagenet classification with deep convolutional neural networks. In *Advances in neural information processing systems*, pages 1097–1105, 2012.
- [19] Zhenzhong Lan, Mingda Chen, Sebastian Goodman, Kevin Gimpel, Piyush Sharma, and Radu Soricut. Albert: A lite bert for self-supervised learning of language representations. *arXiv preprint arXiv:1909.11942*, 2019.
- [20] Vadim Lebedev, Yaroslav Ganin, Maksim Rakhuba, Ivan Oseledets, and Victor Lempitsky. Speeding-up convolutional neural networks using fine-tuned cp-decomposition. *arXiv preprint arXiv:1412.6553*, 2014.
- [21] Hao Li, Asim Kadav, Igor Durdanovic, Hanan Samet, and Hans Peter Graf. Pruning filters for efficient convnets. *arXiv preprint arXiv:1608.08710*, 2016.
- [22] Hanxiao Liu, Karen Simonyan, and Yiming Yang. Darts: Differentiable architecture search. *arXiv preprint arXiv:1806.09055*, 2018.
- [23] Zhuang Liu, Jianguo Li, Zhiqiang Shen, Gao Huang, Shoumeng Yan, and Changshui Zhang. Learning efficient convolutional networks through network slimming. In *Computer Vision (ICCV), 2017 IEEE International Conference on*, pages 2755–2763. IEEE, 2017.
- [24] Jonathan Long, Evan Shelhamer, and Trevor Darrell. Fully convolutional networks for semantic segmentation. In *Proceedings of the IEEE conference on computer vision and pattern recognition*, pages 3431–3440, 2015.
- [25] Jian-Hao Luo, Jianxin Wu, and Weiyao Lin. Thinet: A filter level pruning method for deep neural network compression. *arXiv preprint arXiv:1707.06342*, 2017.
- [26] Neal Parikh, Stephen Boyd, et al. Proximal algorithms. *Foundations and Trends® in Optimization*, 1(3):127–239, 2014.
- [27] Mohammad Rastegari, Vicente Ordonez, Joseph Redmon, and Ali Farhadi. Xnor-net: Imagenet classification

- using binary convolutional neural networks. In *European Conference on Computer Vision*, pages 525–542. Springer, 2016.
- [28] Karen Simonyan and Andrew Zisserman. Two-stream convolutional networks for action recognition in videos. In *Advances in neural information processing systems*, pages 568–576, 2014.
- [29] Shashank Singh, Ashish Khetan, and Zohar Karnin. Darc: Differentiable architecture compression. *arXiv preprint arXiv:1905.08170*, 2019.
- [30] Suraj Srinivas, Akshayvarun Subramanya, and R Venkatesh Babu. Training sparse neural networks. In *2017 IEEE Conference on Computer Vision and Pattern Recognition Workshops (CVPRW)*, pages 455–462. IEEE, 2017.
- [31] Cheng Tai, Tong Xiao, Yi Zhang, Xiaogang Wang, et al. Convolutional neural networks with low-rank regularization. *arXiv preprint arXiv:1511.06067*, 2015.
- [32] Oriol Vinyals, Alexander Toshev, Samy Bengio, and Dumitru Erhan. Show and tell: A neural image caption generator. In *Proceedings of the IEEE conference on computer vision and pattern recognition*, pages 3156–3164, 2015.
- [33] Wei Wen, Chunpeng Wu, Yandan Wang, Yiran Chen, and Hai Li. Learning structured sparsity in deep neural networks. In *Advances in Neural Information Processing Systems*, pages 2074–2082, 2016.
- [34] Chenzhuo Zhu, Song Han, Huizi Mao, and William J Dally. Trained ternary quantization. *arXiv preprint arXiv:1612.01064*, 2016.
- [35] Zhuangwei Zhuang, Mingkui Tan, Bohan Zhuang, Jing Liu, Yong Guo, Qingyao Wu, Junzhou Huang, and Jinhui Zhu. Discrimination-aware channel pruning for deep neural networks. In *Advances in Neural Information Processing Systems*, pages 883–894, 2018.